

## Carotenoid Oxidation in Photosystem II: 1D- and 2D-Electron Spin–Echo Envelope Modulation Study

Y. Deligiannakis,<sup>\*,†,‡</sup> J. Hanley,<sup>‡</sup> and A. W. Rutherford<sup>‡</sup>

*Institute of Materials Science, NCSR “Democritos”  
15310 Aghia Paraskevi Attikis, Greece  
Section de Bioénergetique, URA CNRS 2096  
DBCMA CEA Saclay, 91191, Gif-sur-Yvette Cedex, France*

Received July 26, 1999

Revised Manuscript Received November 8, 1999

Photosystem II (PSII) is the membrane-bound protein complex that catalyzes light-driven electron transfer from water to plastoquinone.<sup>1</sup> It has recently been shown that carotenoid cation radical ( $\text{Car}^+$ ) can be formed stoichiometrically in PS II under illumination at 20 K.<sup>2</sup>  $\text{Car}^+$  is reduced by electron donation from a monomeric chlorophyll ( $\text{Chl}_2$ ) and probably by cytochrome  $b_{559}$ .<sup>2</sup> Thus it is thought that carotenoid plays an important role as an electron carrier in a pathway that provides electrons to the ultrareactive photooxidized chlorophyll cation  $\text{P680}^+$ , under those conditions where electrons from the water oxidizing system are limiting<sup>2</sup> (see also ref 3). Given this new redox role, attention has now focused on the spectroscopy of carotenoid.<sup>4</sup> To obtain information on its protein environment, we have performed electron spin–echo envelope modulation (ESEEM)<sup>6</sup> spectroscopy on  $\text{Car}^+$  in PSII. Recently ESEEM has provided important information about the amino acid environment of the semiquinone radicals in photosystem II,<sup>8a–c</sup> in photosystem I,<sup>8d</sup> and in a bacterial reaction center.<sup>8e,f</sup> In addition, two-dimensional hyperfine sublevel correlation spectroscopy (HYSCORE)<sup>7</sup> has proven to be a powerful tool for resolving complicated ESEEM spectra.<sup>9,10</sup> Here, based on HYSCORE together with numerical simulations, the observed modulations are shown to originate from a single protein  $^{14}\text{N}$  nucleus assigned to the indole nitrogen of a tryptophan residue in PSII.

<sup>†</sup> NCSR Democritos.

<sup>‡</sup> Section de Bioénergetique.

(1) Diner, B. A.; Babcock, G. T. In *Oxygenic Photosynthesis: the light reactions*; Ort, D. R., Yocum, C. F., Eds.; Kluwer: Dordrecht, 1996; pp 213–247.

(2) Hanley, J.; Deligiannakis, Y.; Pascal, A.; Faller, P.; Rutherford, A. W. *Biochemistry* **1999**, *38*, 8195.

(3) (a) Thompson, L. K.; Diner, B. A.; Brudvig, G. W. *Biochemistry* **1988**, *27*, 6653. (b) Buser, C. A.; Diner, B. A.; Brudvig, G. W. *Biochemistry* **1992**, *31*, 1149.

(4) Some vibrational spectroscopic studies have already been done on the carotenoid cation in PSII.<sup>5</sup>

(5) (a) Noguchi, T.; Mitsuka, T.; Inoue, Y. *FEBS Lett.* **1994**, *356*, 179. (b) Pascal, A.; Telfer, A.; Barber, J.; Robert, B. *FEBS Lett.* **1999**, *453*, 11. (c) Vrettos, J. S.; Stewart, D. H.; Gaa, A.; DePaula, J. C.; Bocian, D. F.; Brudvig, G. W. *Biophys J.* **1999**, *76*, A248.

(6) Dikanov, S. A.; Tsvetkov, Y. D. *ESEEM Spectroscopy*; CRC Press: Boca Raton, FL 1992.

(7) Höfer, P.; Grupp, H.; Nedenführ, M.; Mehring, *Chem. Phys. Lett.* **1986**, *132*, 279.

(8) (a) Deligiannakis, Y.; Boussac, A.; Rutherford, A. W. *Biochemistry* **1995**, *34*, 16030. (b) Deligiannakis, Y.; Jegerschöld, C.; Rutherford, A. W. *Chem. Phys. Lett.* **1997**, *270*, 564. (c) Astashkin, A. V.; Kawamori, A.; Kodera, Y.; Kuroiwa, S.; Akabori, K. **1998** *J. Chem. Phys.* *102*, 5583. (d) Hanley, J.; Deligiannakis, Y.; MacMillan F.; Bottin, H.; Rutherford, A. W. *Biochemistry* **1997**, *36*, 11544. (e) Spoyalov, A. P.; Huslbesbosch, R. J.; Shochat, S.; Gast, P.; Hoff A. J. *Chem. Phys. Lett.* **1996**, *263*, 715. (f) Lentzian, F.; Rautter, G.; Käβ, H.; Gardiner, A.; Lubitz, W. *Ber. Bunsen-Ges. Phys. Chem.* **1996**, *100*, 2036.

(9) (a) Deligiannakis, Y.; Rutherford, A. W. *J. Am. Chem. Soc.* **1997**, *119*, 4471. (b) Dikanov, S. A.; Davydov, R. M.; Gräslund, A.; Bowman, M. K. *J. Am. Chem. Soc.* **1998**, *120*, 6797. (c) Tyryshkin, A. M.; Dikanov, S. A.; Reijerse, E. J.; Bughard, C.; Huettermann, J. *J. Am. Chem. Soc.* **1999**, *121*, 3396. (d) Dikanov, S. A.; Xun, L.; Karpel, A. B.; Tyryshkin, A. M.; Bowman, M. K. *J. Am. Chem. Soc.* **1996**, *118*, 8408.

(10) Deligiannakis, Y.; Hanley, J.; Rutherford, A. W. *J. Am. Chem. Soc.* **1999**, *121*, 7653.

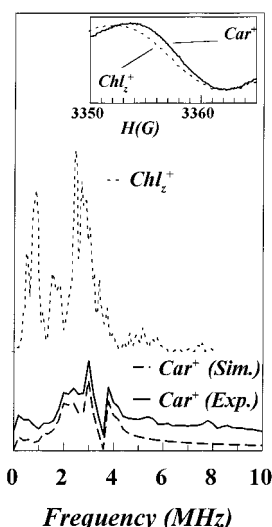


**Figure 1.** FT 3p-ESEEM for  $\text{Car}^+$  radical in PSII (solid line). Experimental conditions: 9.64 GHz, 3450 G, 26 K,  $\tau = 104$  ns, time interval between successive pulse sets 10 ms. The simulated spectrum (dashed line) was calculated for one  $^{14}\text{N}(I = 1)$  nucleus with  $\mathbf{A} = (A_x, A_y, A_z) = (0.6 \pm 0.1, 0.6 \pm 0.1, 0.8 \pm 0.1)$  MHz,  $(\alpha, \beta, \gamma) = (0^\circ, 50^\circ \pm 15^\circ, 0^\circ)$ , and  $e^2qQ/h = 3.09 \pm 0.08$  MHz,  $\eta = 0.18 \pm 0.10$ . Inset: CW EPR spectrum of the  $\text{Car}^+$  radical in PSII (solid line). The CW EPR and 3p-ESEEM spectra of the  $\text{Chl}_2^+$  radical are also displayed for comparison (dotted lines).

The  $\text{Car}^+$  radical accumulated by illumination of Mn-depleted PSII membranes at 20 K<sup>2</sup> is characterized by a continuous wave EPR spectrum shown in the inset of Figure 1 (solid line). At higher temperatures the  $\text{Car}^+$  is reduced through electron donation from  $\text{Chl}_2$ , forming the chlorophyll cation radical,  $\text{Chl}_2^+$ . The EPR signals from these two radicals are very similar; indeed, until recently the  $\text{Car}^+$  signal was misassigned as  $\text{Chl}_2^+$ . In the inset of Figure 1, the spectrum of  $\text{Chl}_2^+$ , selectively photoaccumulated by illumination at 200 K<sup>2</sup>, is shown as a broken line. It was shown earlier that the  $\text{Car}^+$  and  $\text{Chl}_2^+$  radicals can be distinguished by their optical spectra.<sup>2,11</sup>

The 3p-ESEEM spectrum for  $\text{Car}^+$  (solid line in Figure 1) is dominated by low-frequency components at 2.2–2.5, 2.9, and 3.8–4.2 MHz. This spectrum is clearly different from the ESEEM spectrum of  $\text{Chl}_2^+$ <sup>13</sup> (Figure 1, dotted line); thus, the ESEEM spectra provide a sensitive probe for distinguishing these radicals in PSII. The HYSCORE spectrum for  $\text{Car}^+$  (Figure 2) is dominated by cross-peaks at 2.4–3.1, 4.0–4.4 MHz with maximum intensity in the (+,+) quadrant. These are assigned<sup>14a</sup> to the  $(\nu^{(3)}_\alpha, \nu^{(3)}_\beta)$  features due to an interacting  $^{14}\text{N}(I = 1)$  nucleus with  $A_{\text{iso}} < 2\nu$ .<sup>9d,10</sup> From the  $\nu^{(3)}_\beta$  frequency, assuming  $K$  values of 0.3–0.8 MHz appropriate for protein nitrogens,<sup>16a</sup> we get an initial estimate of  $A_{\text{iso}}$  which is further refined by numerical simulations of the 3p-ESEEM; accordingly, the ESEEM for  $\text{Car}^+$  is well simulated<sup>14b</sup> (Figure 1, dashed line) by assuming one  $^{14}\text{N}$  nucleus with  $\mathbf{A} = (A_x, A_y, A_z) = (0.6, 0.6, 0.8)$  MHz,  $e^2qQ/h = 3.09$  MHz, and  $\eta = 0.18$  MHz.

The present ESEEM data show that the  $\text{Car}^+$  radical of PSII interacts with one protein  $^{14}\text{N}$  nucleus. Based on previous NQR<sup>16b</sup>

(11)  $\text{Car}^+$  formation in PSII was reported earlier using electron absorption spectroscopy in the visible and near-infrared regions;<sup>5a,12</sup> however, its stoichiometry and its role in electron transfer were demonstrated only recently.<sup>2</sup>

(12) (a) Velthuys, B. R. *FEBS Lett.* **1981**, *126*, 272. (b) Schenk, C. C.; Diner, B. A.; Mathis, P.; Satoh, K. *Biochim. Biophys. Acta* **1982**, *680*, 216.

(13) The 3p-ESEEM for the  $\text{Chl}_2^+$  (Figure 1) is dominated by features at 0.6–1.0, 1.6–1.8, 2.4–3.1, and 5.0–6.0 MHz; these originate mainly from the pyrrole  $^{14}\text{N}$  of the  $\text{Chl}_2$  (Deligiannakis, Y.; et al., in preparation).

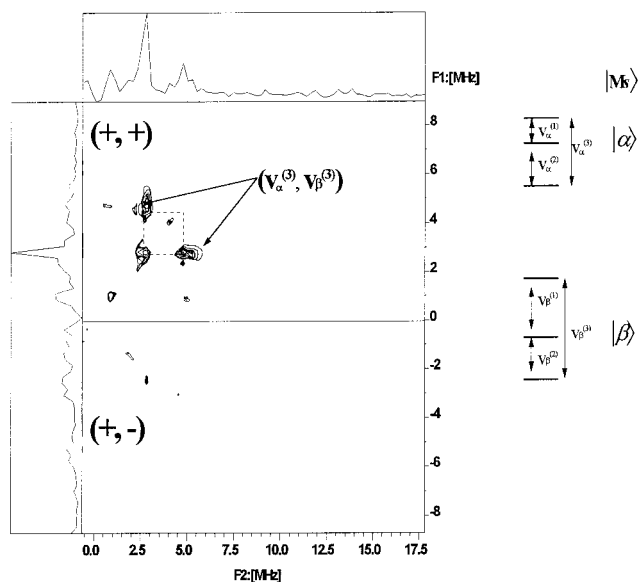


**Figure 2.** Experimental 2D-HYSCORE spectrum (contour plots) for  $\text{Car}^+$  radical in PSII recorded at  $\tau = 168$  ns with  $H = 3456$  G. Experimental conditions:  $t_1 t_2 = 256 \times 256$  points; start values,  $t_1 = 40$  ns,  $t_2 = 140$  ns;  $T = 24$  K. Other conditions are as in Figure 1. The nuclear transitions for a  $^{14}\text{N}$  ( $I = 1$ ) nucleus coupled to  $S = 1/2$  are displayed on the right side.

and ESEEM<sup>8f</sup> data, the  $e^2qQ/h$  and  $\eta$  values for this nucleus (3.09 MHz, 0.18) are assigned<sup>16c</sup> to the indole  $^{14}\text{N}$  of a tryptophan residue. With the current state of knowledge it is not possible to assign which tryptophan in the PSII reaction center is responsible for this coupling. However, it is of interest to look to the purple bacterial reaction center for insights since it has been shown that the other PSII cofactors (other than the Mn cluster and the cytochrome b559 heme) have structural counterparts in the bacterial reaction center.<sup>1</sup>

In the bacterial reaction center, the carotenoid is located in the M subunit, is in van der Waals contact with the monomeric

(14) (a) For one  $^{14}\text{N}$  ( $I = 1$ ) nucleus coupled to an  $S = 1/2$  spin, the energy level scheme is given in Figure 2. For weak coupling  $A_{\text{iso}} < 2\nu_1$ , in the intermediate deviation from the cancellation condition<sup>15</sup>  $|\nu_1 - A_{\text{iso}}/2| < 4K/3$ , the HYSCORE spectrum is dominated by cross-peaks at  $(\nu^{(3)}_{\alpha}, \nu^{(3)}_{\beta})$  in the (+, +) quadrant (for details, see ref 9d). Cross-peaks, assignable to  $(\nu^{(1)}_{\alpha}, \nu^{(3)}_{\beta})$ , can be resolved in certain HYSCORE spectra of  $\text{Car}^+$ ; however, these are very weak, and the  $\nu^{(1)}_{\alpha}$  position can be estimated only within the limit  $\sim 0.3$ – $0.7$  MHz. (b) The analysis of the data is as follows: from the frequency  $\nu^{(3)}_{\beta}$  we get an initial estimate of possible  $A_{\text{iso}}$  values. The shape of the HYSCORE peaks implies (see refs 9a,d, 10) that the hyperfine anisotropy is small when compared with  $A_{\text{iso}}$ . Starting with these estimates and limitations, the 3p-ESEEM spectra for  $\text{Car}^+$  were simulated at several  $\tau$  values. The Euler angle  $\beta$  was then adjusted to get the best simulation of the relative intensities; angles  $\alpha$  and  $\gamma$  are set arbitrarily equal to zero.

(15) Flanagan, H. L.; Singel, D. J. *J. Chem. Phys.* **1987**, *87*, 5606.

(16) (a) Edmonds, D. T. *Phys. Rep.* **1977**, *C29*, 233. (b) Pertinent ( $e^2qQ/h$ ,  $\eta$ ) values for amino acid  $^{14}\text{N}$ -nuclei are 3.45 MHz and 0.45 for backbone amide nitrogen, 3.27 MHz and 0.14 for amino nitrogen of imidazole ring, 3.36 MHz and 0.13 for imidazole in L-histidine, and 3.10 MHz and 0.18 in indole. (c) In the present case, due to the weak  $A_{\text{iso}}$ , the spectrum is sensitive to the quadrupole interaction, especially on  $e^2qQ/h$  and to a lesser extent on  $\eta$ , and this allows credible estimation of the quadrupole parameters. The value  $e^2qQ/h = 3.09 \pm 0.08$  MHz found for  $\text{Car}^+$  is indicative of an indole  $^{14}\text{N}$ .

bacterial chlorophyll on that side of the reaction center, has a 15,15'-cis conformation, and spans only a small fraction of the membrane.<sup>17,18</sup> Significantly, the carotenoid binding pocket in *Rhodobacter sphaeroides* is lined by five tryptophan residues (M66, M75, M115, M157, and M171).<sup>17</sup> Among them, TrpM157 has its indole nitrogen located over the ( $\text{C}_{13}$ )– $\text{C}_{\beta}\text{H}_3$  methyl group of the carotenoid,<sup>17</sup>  $R_{[\text{N}(\text{indole}(\text{TrpM157})-\text{C}_{\beta}(\text{C}_{13}))]} = 4.82$  Å. This methyl group (along with that in the C13' position) bears the highest unpaired electron spin density in the  $\text{Car}^+$  in vitro.<sup>19</sup> Furthermore, recent resonance Raman/site-directed mutagenesis studies in the *R. sphaeroides* reaction center showed that tryptophans M115 and M157<sup>20</sup> affected the geometry of the central 15,15' bond and the effective conjugation length of the carotenoid, possibly due to an increased distortion from the planar geometry along its C=C backbone.<sup>20</sup>

In principle, homologous tryptophan residues in the PSII reaction center (e.g., D2 112 and D2 168, homologous to M115 and M171, respectively, and D2 49 and D2 59, which may be homologous to M66 and M75, respectively)<sup>21</sup> are potential candidates for the origin of interacting indole  $^{14}\text{N}$  reported here. Although these groups may provide a starting point for site-directed mutagenesis experiments aimed at identifying the carotenoid-associated tryptophan, it should be pointed out that the functional differences reported for carotenoid in the two different types of reaction centers likely reflect significant structural differences.<sup>22,23</sup> At this time, then, the main insight gained from examination of the situation in the bacterial reaction center is that tryptophan residues seem to play a key role in the carotenoid binding site. In PSII, the tryptophan seems to be even more closely associated with the carotenoid than is the case in the bacterial reaction center. This interaction, then, may well have a significant influence on the electronic properties of the carotenoid and may thus play an important role in terms of its redox activity as well as its structure.

**Acknowledgment.** We thank P. Faller and A. Pascal for useful discussion. This work was supported by the TMR Grants FMRX-CT 96-0031 and FMRX-CT98-0214

JA9926257

(17) Ermler, U.; Fritsch, G.; Buchanan, S. K.; Michel, H. *Structure* **1994**, *2*, 925.

(18) Frank, H. In *The Photosynthetic Reaction Center*; Deisenhofer, J., Norris, J. R., Eds.; Academic Press: San Diego, CA, 1993; Vol. II, pp 221–235.

(19) (a) Piekara-Sady, L.; Khaled, M. M.; Bradford, E.; Kispert, L. D.; Plato, M. *Chem. Phys. Lett.* **1991**, *186*, 143. (b) Piekara-Sady, L.; Jeevarajan, A. S.; Kispert, L. D. *Chem. Phys. Lett.* **1993**, *207*, 173. (c) Jeevarajan, A. S.; Kispert, L. D.; Piekara-Sady, L. *Chem. Phys. Lett.* **1993**, *209*, 269.

(20) Gall, A.; Ridge, J. P.; Robert, B.; Cogdell, R.; Jones, M. R.; Fyfe, P. K. *Photosynth. Res.* **1999**, *59*, 223.

(21) These conclusions are based on sequence alignments of *R. sphaeroides* with the PSII reaction center proteins (Satoh, K. In *The Photosynthetic Reaction Center*; Deisenhofer, J., Norris, J. R., Eds.; Academic Press: San Diego, CA, 1993; Vol. I, pp 289–318). We note that no tryptophans are present in equivalent regions of D1.

(22) The carotenoid in PSII appears to be unable to quench the  $\text{P}_{680}$  triplet state, while in bacterial reaction centers the equivalent reaction is efficient.<sup>18</sup> The oxidation of carotenoid by  $\text{P}_{680}^+$  and its proposed reduction by Cyt b559 indicate that the carotenoid has an extended structure (see also ref 23) and spans a significant proportion of the membrane.<sup>2</sup>

(23) Yruela, I.; Tomas, R.; Sanjuan, M.; Torrado, E.; Aured, M.; and Picorel, R. *Photochem. Photobiol.* **1998**, *68*, 729.